► Transport of Droplets by Thermal Capillarity
► Wetting and Spreading

References

1. Yih CH (1995) Kinetic-energy mass, momentum mass, and drift mass in steady irrotational subsonic flow. J Fluid Mechanics 297:29–36
2. Huang W, Bhullar RS, Fung YC (2001) The surface-tension-driven flow of blood from a droplet into a capillary tube. ASME J Biomedical Eng 123:446–454
3. Chakraborty S (2005) Dynamics of capillary flow of blood into a microfluidic channel. Lab Chip 5:421–430
4. Law HS, Fung YC (1970) Entry flow into blood vessels at arbitrary Reynolds number. J Biomechanics 3:23–38
5. Hoffman RL (1975) A study of the advancing interface I. Interface shape in liquid-gas systems. J Colloid Interface Sci 50:228–235
6. Sheng P, Zhou M (1992) Immiscible-fluid displacement: contact-line dynamics and the velocity-dependent capillary pressure. Phys Rev A 45:5694–5708
7. Tso CP, Sundaravadivelu K (2001) Capillary flow between parallel plates in the presence of an electromagnetic field. J Phys D 34:3522–3527
8. Yang J, Lu F, Kwok DY (2004) Dynamic interfacial effect of electroosmotic slip flow with a moving capillary front in hydrophobic circular microchannels. J Chem Phys 121:7443–7448
9. Yang L-J, Yao T-J, Tai Y-C (2004) The marching velocity of the capillary meniscus in a microchannel. J Micromech Microeng 14:220–225
10. Tas NR, Haneveld J, Jansen HV, Elwenapoek, van den Berg A (2004) Capillary filling speed of water in nanochannels. Appl Phys Lett 18:3274–3276

Capillary Flow

► Surface Tension Driven Flow

Capillary Force Valves

DANIEL IRIMIA
Massachusetts General Hospital,
Harvard Medical School, Boston, MA, USA
dirimia@partners.org

Synonyms

Capillary valves

Definition

Capillary force valves are fluid control structures that use superficial tension at the interface between different fluids to block and/or restore the entrance of fluids in microchannels filled with a second immiscible fluid. For most of the microfluidic applications the second fluid is air, and the liquid–air interface at a narrow hydrophobic stricture is used to prevent the liquid from entering a capillary.

Overview

Capillary forces result from the interaction of liquid, gas and solid surfaces, at the interface between them. In the liquid phase, molecules are held together by cohesive forces. In the bulk of the liquid, the cohesive forces between one molecule and the surrounding molecules are balanced. However, for the same molecule at the edge of the liquid, the cohesive forces with other liquid molecules are larger than the interaction with air molecules (Fig. 1). As a result, the liquid molecules at the interface are pulled together towards the liquid. The overall effect of these forces is to minimize the free surface of the liquid that is exposed to air. The proportionality between the decrease in energy of the surface that results from decreasing the surface is described by the *surface tension*:

$$\gamma = \frac{dG}{dA}$$

where dG is the change in energy [N m], dA is the change in area [m^2] and γ is the surface tension or surface energy [N/m].

Of interest for capillary forces is the contact between three phases: liquid, solid and vapor (air). Three forces are present, trying simultaneously to minimize the contact area between the three phases. At equilibrium, the forces at the triple interface are balanced (Fig. 2) and the relationship between them is described by the Young–Dupree

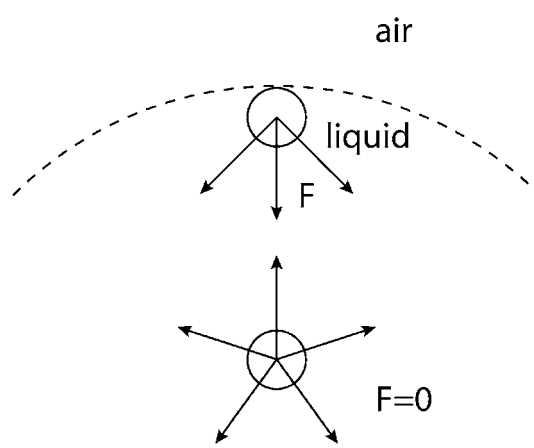

Capillary Force Valves, Figure 1 Superficial tension forces at the interface between a liquid and air. For molecules in the liquid there is a balance of the cohesive forces ($F = 0$), while for molecules closer to the interface, the cohesive forces with other molecules in the liquid are larger than the interaction with air molecules (resultant force F towards the bulk of the liquid)

equation:

$$\gamma_{AS}L = \gamma_{LS}L + \gamma_{LA}L \times \cos\Theta$$

where L is the length of the triple contact line and Θ is the contact angle between the liquid and the solid. It is interesting to observe the vertical component pulling on the solid surface in the case of wetting and pushing in the case of non-wetting surfaces.

Capillary forces are critical at the microscale. The surface tension is responsible for the increased pressure in a bubble trapped in a capillary, and for the increased pressure required to push liquid into an empty non-wetting capillary (Fig. 3). The relation between surface tension and pressure is given by the Laplace equation:

$$\Delta P = \gamma C$$

where C is the curvature of the liquid surface. Depending of the shape of the capillary, different formulas for the curvature are available:

$$C = \frac{2}{R}$$

$$C = \frac{1}{R_1} + \frac{1}{R_2}$$

where R is the curvature radius for the liquid in a circular capillary and R_1 and R_2 are the curvatures in a non-circular capillary.

Basic Methodology

The behavior of air and liquids in capillaries is of critical importance at the microscale. After their fabrication, most of the channels in microfluidic devices are filled with air. In general, before the microfluidic devices are used for their designed purpose, the air inside the microfluidic channels has to be replaced by the working fluid. However, there are many applications where not all the air is replaced at once, and the advance of fluid inside the microfluidic channels is controlled through capillary force valves.

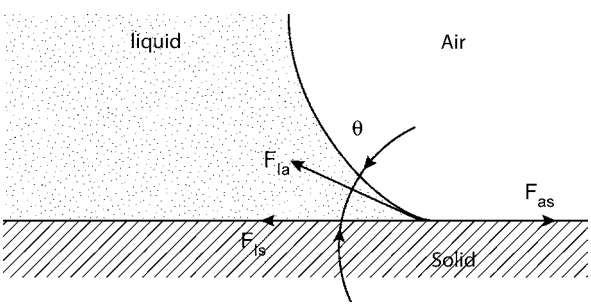

Capillary Force Valves, Figure 2 Capillary forces at the interaction between air, liquid and solid surfaces. Each of these forces works to minimize the energy of the interface between liquid and solid, air and solid, liquid and air: F_{ls}, F_{as}, F_{la}, respectively. At equilibrium, the horizontal projection of F_{la} and F_{ls} and F_{as} cancel each other. The corresponding angle between F_{la} and F_{ls} is the contact angle between liquid and solid (Θ)

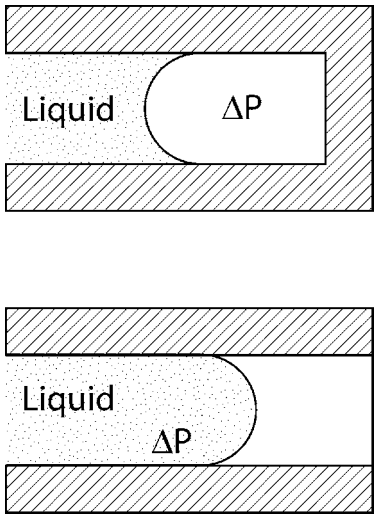

Capillary Force Valves, Figure 3 Capillary forces in hydrophilic capillaries result in increased pressure in trapped air bubbles. Capillary forces in hydrophobic capillaries prevent liquid from entering the capillary, and can be overcome by larger pressure

Two major strategies for making valves using the capillary forces are through the use of (a) local changes of contact angle and (b) local changes of surface geometry.

(a) The use of hydrophobic patches in a capillary relies on the increased pressure that is required to push the liquid over the area of larger contact angle (Fig. 4). The increased contact angle between the liquid and the capillary in the region of the hydrophobic patch results in a larger pressure necessary for moving the liquid over that region. After passing the patch, the pressure required for moving the liquid returns to pre-patch values. The combination of hydrophobic patches on the bottom of the channel is of interest for microfluidic devices where precise valving is required, or for liquids with different characteristics.

One other particular effect of practical interest whenever capillary forces are used is the difference between advancing and receding angles for the same fluid in the same capillary. This phenomenon is also known as hysteresis and manifests itself as larger contact angle at the advancing edge of a liquid–solid interface compared to the equilibrium contact angle which is itself larger than the contact angle at the receding edge of the liquid–solid interface (Fig. 5). The origin of this is partially in the roughness of the surface and can have interesting effects when moving columns of liquids through capillaries [1].

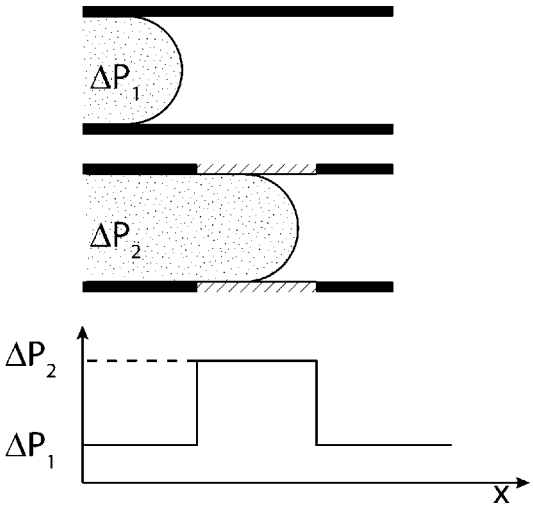

Capillary Force Valves, Figure 4 Schematics of a capillary valve using a hydrophobic patch. The pressure required to move the liquid (ΔP_1) is higher when the liquid–air interface reaches the region of increased hydrophobicity (ΔP_2)

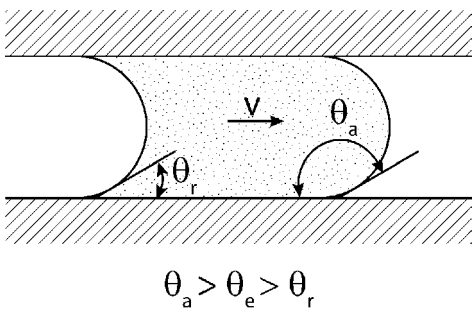

Capillary Force Valves, Figure 5 Hysteresis in contact angle. The contact angle at the advancing interface (Θ_a) is usually larger than the equilibrium contact angle (Θ_e), and larger than the contact angle at the trailing interface (Θ_t)

(b) The larger contact angle at advancing interfaces can be used in capillary valves as well, in combination with local change of the shape of the surface or the change in the diameter of the capillary (Fig. 6). This approach to controlling a liquid–air interface can be used alone or in combination with the hydrophobic patches. Although the fluid control is usually less precise for valves using changes in diameter compared to valves using hydrophobic patches, their implementation in microfluidic devices is overall easier.

Key Research Findings

For the majority of microfluidic devices the initial filling (priming) of the device with liquid or the formation of air bubbles inside can render the device unusable. However,

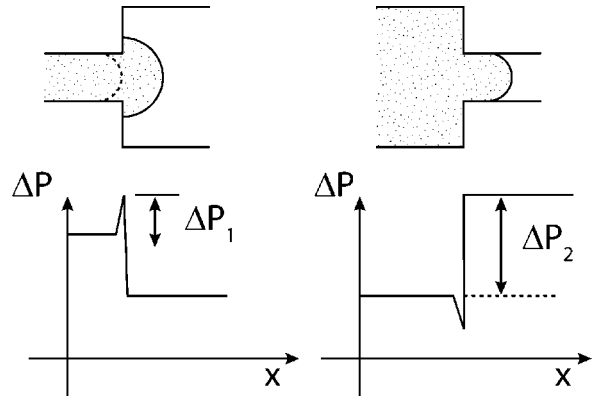

Capillary Force Valves, Figure 6 Schematics of capillary valves using changes in the diameter of the capillary. Rapid enlargement of a capillary changes the physical angle between the liquid interface and the solid surface and can form a temporary barrier for the advancing liquid (ΔP_1). Reducing the diameter of a hydrophobic capillary reduces the radius of curvature of the interface and requires larger pressure (ΔP_2) to move the liquid and could also function as a valving mechanism

there are numerous examples that use the liquid–air interfaces to control the flow of liquid for different applications. Wall-less control of the flow of liquid streams has been demonstrated on micropatterned hydrophobic surfaces (Fig. 7) [2]. Micropatterned patches have been used to precisely stop the liquid flow at a certain position inside a channel without the need for moving parts (Fig. 8) [3], and for the accurate metering of nanoliter volumes of liquids in microchannels [4, 5]. Handling of minute volumes of fluids and mixing inside a capillary have been reported. Through the use of passive valves to control the flow of fluid and air bubbles expanded from side chambers, volumes of liquids down to 25 pL can be handled precisely (Fig. 9) [6]. The hydrophobic nature of the liquid–wall interaction was critical for stable and complete separation of picoliter volumes of fluid [7].

Capillary valves are burst valves, i. e. once the liquid passes through them they no longer function as valves. Resetting a capillary valve requires the formation of the liquid–liquid or liquid–gas interface at the location of hydrophobic interaction. This can be achieved by the injection of gas or liquid, usually in a small volume, from a reservoir or generated on the chip [6, 8].

Future Directions for Research

Capillary valves have no moving parts, are simple and easy to implement and thus are very attractive for low-cost microfluidic devices. At the same time, several areas of improvement are under scrutiny, to increase the performance of the valve, to improve the integration and to

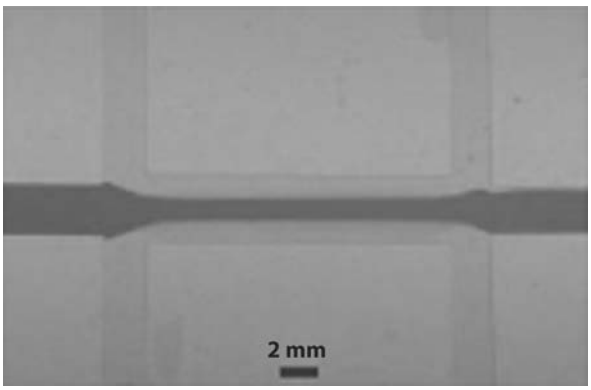

Capillary Force Valves, Figure 7 Hydrophilic and hydrophobic patches are used to control the flow of liquid streams (here rhodamine in water) in a wall-less configuration, just by relying on the surface tension of the liquid [2] (▶ Color Plate 11)

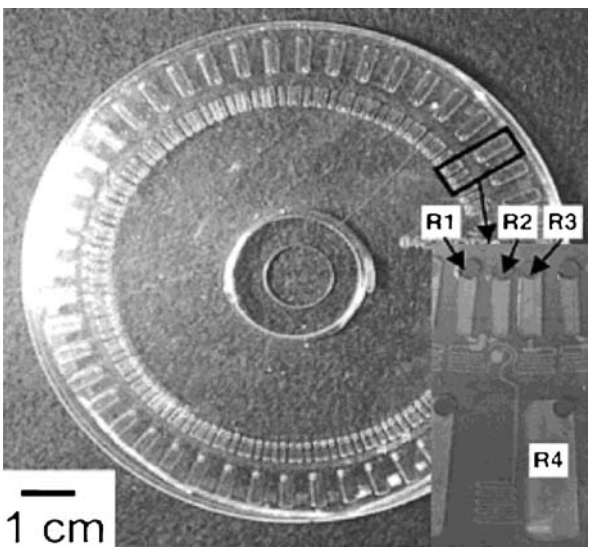

Capillary Force Valves, Figure 8 Capillary burst valves are used to control the sequential mixing of reagents in a Lab-on-a-CD type device. The solutions of enzyme, inhibitor and substrate were loaded in reservoirs that were connected to channels labeled R1, R2 and R3, respectively. R4 is a reservoir for waste collection. The rotation of the disk at different speeds controls the opening of the valves, and the sequence of mixing the enzyme with the inhibitor, followed by mixing with the substrate, and detection [3]

expand the range of applications. Continuous efforts are made to enlarge the variety of liquids that can be handled by new approaches to surface patterning in microcapillaries. The integration of an increasing number of valves for the implementation of complex reaction protocols is also an area of active research, especially, but not limited to, Lab-on-a-CD type devices [9]. Finally, while microfluidic devices are developed for applications outside the laboratory, it becomes increasingly important to

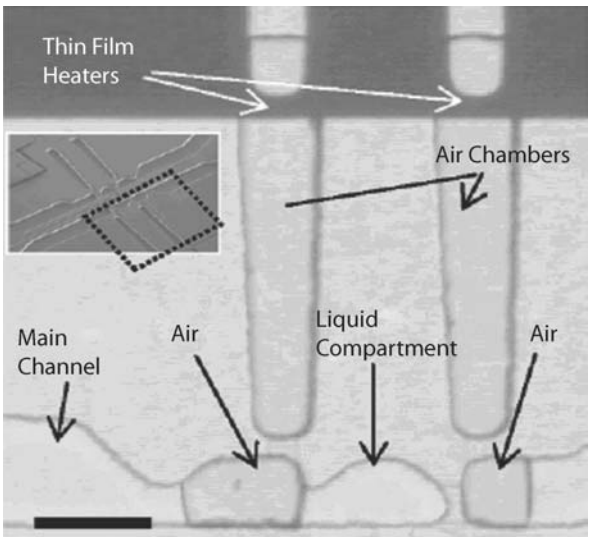

Capillary Force Valves, Figure 9 A volume of 25 pL is isolated by the creation of two new liquid–air interfaces, through the use of two thermal actuators. Two air bubbles isolate the separated volume from the rest of the liquid in the main channel [6] (▶ Color Plate 19)

provide robust valve designs that would ensure functioning over a wider range of temperatures, storage conditions and operator training, etc.

Cross References

- ▶ Lab-on-a-Chip (General Philosophy)
- ▶ Centrifugal Microfluidics
- ▶ Applications Based on Electrowetting
- ▶ Electrowetting
- ▶ Biosample Preparation Lab-on-a-Chip Devices
- ▶ Boiling and Evaporation in Microchannels
- ▶ Bubble Actuated Microfluidic Switch
- ▶ Capillary Filling
- ▶ Control of Microfluidics
- ▶ Droplet and Bubble Formation in Microchannels
- ▶ Electrocapillary
- ▶ Electrochemical Valves
- ▶ Electrowetting
- ▶ Fabrication of 3D Microfluidic Structures
- ▶ Fluid Metering
- ▶ Integrated Microfluidic Systems for Medical Diagnostics
- ▶ Lab-on-Chip Devices for Chemical Analysis
- ▶ Marangoni Convection
- ▶ Microfluidic Circuits
- ▶ Microfluidic Sample Manipulation
- ▶ Surface Tension, Capillarity and Contact Angle
- ▶ Transport of Droplets by Thermal Capillarity
- ▶ Water Management in Micro DMFCs

References

1. de Gennes P-G, Brochard-Wyart F, Quéré D (2004) Capillarity and wetting phenomena: drops, bubbles, pearls, waves; translated by Axel Reisinger. Springer, New York
2. Zhao B, Moore JS, Beebe DJ (2001) Surface-directed liquid flow inside microchannels. Science 291:1023–1026
3. Duffy DC, Gillis HL, Lin J, Sheppard NF, Kellogg GJ (1999) Microfabricated Centrifugal Microfluidic Systems: Characterization and Multiple Enzymatic Assays. Anal Chem 71:4669–4678
4. Handique K, Burke DT, Mastrangelo CH, Burns MA (2001) On-chip thermopneumatic pressure for discrete drop pumping. Anal Chem 73:1831–1838
5. Lee SH, Lee CS, Kim BG, Kim YK (2003) Quantitatively controlled nanoliter liquid manipulation using hydrophobic valving and control of surface wettability. J Micromech Microeng 13:89–97
6. Irimia D, Tompkins RG, Toner M (2004) Single-cell chemical lysis in picoliter-scale closed volumes using a microfabricated device. Anal Chem 76:6137–6143
7. Ajaev VS, Homsy GM (2001) Steady Vapor Bubbles in Rectangular Microchannels. J Colloid Interface Sci 240:259–271
8. Oh KW, Ahn CH (2006) A review of microvalves. J Micromech Microeng 16:R13–R39
9. Madou M, Zoval J, Jia G, Kido H, Kim J, Kim N (2006) Lab on a CD. Annu Rev Biomed Eng 8:601–628

Capillary Magnetophoresis

► Magnetophoresis

Capillary Reactor

► Droplet Microreactor

Capillary Valves

► Capillary Force Valves

Capillary Zone Electrophoresis

► Capillary Electrophoresis

Caspase Activation

► Microfluidics for Studies of Apoptosis

Cast-in-Place Polymeric Media

► Stationary Phases in Microchannels

Catalyst Testing

Definition

A branch of combinatorial chemistry used for developin develop in an empirical or semi-empirical manner new and more efficient catalysts.
Most often, in the heterogeneous catalysis the catalysts are solids–usually metals, very often precious metals–while the reactants are liquid or gaseous. The catalysts are usually composed of a number of (metal) components in various combinations. The tests are performed in parallel under the otherwise equal temperature and pressure conditions in a large number of microreactors. In each microreactor the combination of the tested catalyst components is different and this results in a different yield or selectivity of the test reaction. This is usually evaluated by composition analysis of the reaction products. The results are stored in a combinatorial library and processed mathematically to determine the optimum combination.

Cross References

► Microfluidic Systems for Combinatorial Chemistry
► Combinatorial Library

Cataphoresis

► Electrokinetic Motion of Cells and Nonpolarizable Particles

Cathode

Definition

Negatively charged electrode.

Cross References

► Electrophoresis

Cathode Sputtering

► Sputtering for Film Deposition

as addressed previously. Min et al. [2] have thoroughly investigated the effect of the three dimensionless parameters on η_{max} based on Eq. (36). They have demonstrated that η_{max} can be increased by decreasing the viscosity or by increasing the dielectric constant of the liquid. They have also proposed the possibility that efficiencies as high as 15% are possible with careful attention to the channel size and the solution composition.

Examples of Application

It has been shown that the thermal efficiency of the electroosmotic pump is very low. Most of the electric energy put into the electrolyte liquid is dissipated into heat, so called Joule heating. In many cases, the mismatch between the theory and the measurement for the pressure is attributed to the Joule heating [5].

The maximum efficiency achievable through a careful selection of packed materials and electrolyte has been reported by Min et al. [2] to be at most 15%. In contrast, Griffiths and Nilson [6] reported that the likely maximum efficiency for any electroosmotic pump would be about 10% for operation at the condition of maximum work.

Hu and Chao [7] performed two-dimensional numerical simulation on the performance of an electroosmotic pump for planar channels. The model is able to handle the case with the dimensions comparable to the EDL thickness. Also no Debye–Huckle approximation and symmetric conditions are required. But the results show considerable deviation from the experimentally measured ones.

Yao and Santiago [8] provided useful review on the historical background of the development of EO pumps. They considered different molar conductivities for cations (Λ_+) and anions (Λ_-) in calculating the electric current caused by electromigration. They predicted that Λ_+ is almost twice Λ_- for sodium ions.

Kang et al. [9] considered the wall effect surrounding the packed materials. Zeta potentials on the inner surface may not be the same as those of packed spheres, and the porosity is a function of the distance from the wall. The wall effect is more enhanced for larger packed particles.

Yao et al. [10] studied an electroosmotic pump made from porous silicon membranes having straight circular pores. Tortuosity is unity and ψ was measured directly from SEM images of the cross-section. Zeta potential is calculated by using the formula for the ratio Q_{max}/I_{max} and the measured data of Q_{max} and I_{max}. Comparison between theory and experiment is good for the plots Q_{max} versus V and I_{max} versus V. There was considerable deviation for the prediction of Δp_{max} and Yao et al. attributed this discrepancy to the problem in the zeta potential measurement and non-uniform distribution of the pore size. At a lower flow rate, the buffer electrolyte shows variation of PH leading to unstable results.

Cross References

- ► Electroosmotic Flow (DC)
- ► Electroosmosis Flow in Heterogeneous Microchannels
- ► AC Electroosmotic Flow
- ► Analysis of Electroosmotic Flow by Lattice–Poisson–Boltzmann Method
- ► Combined Pressure-Driven Flow and Electroosmotic Flow
- ► Electrokinetic Flow in Porous Media
- ► Electrokinetic Sample Injection

References

1. Li D (2004) Electrokinetics in Microfluidics. Elsevier Academic Press
2. Min JY, Hasselbrink EF, Kim SJ (2004) On the efficiency of electrokinetic pumping of liquids through nanoscale channels. Sens Actuators B 98:368–377
3. Wang C, Wong TN, Yang C, Ooi KT (2007) Characterization of electroosmotic flow in rectangular microchannels. Int J Heat Mass Transfer 50:3115–3121
4. Zeng S, Chen C-H, Mikkelsen Jr. JC, Santiago JG (2001) Fabrication and characterization of electroosmotic micropump. Sens Actuators B 79:107–114
5. Morf WE, Guenat OT, de Rooij NF (2001) Partial electroosmotic pumping in complex capillary systems Part 1: principles and general theoretical approach. Sens Actuators B 72:266–272
6. Griffiths SK, Nilson RH (2005) The efficiency of electrokinetic pumping at a condition of maximum work. Electrophoresis 26:351–361
7. Hu JS, Chao CYH (2007) A study of the performance of microfabricated electroosmotic pump. Sens Actuators A 135:273–282
8. Yao S, Santiago JG (2003) Porous glass electroosmotic pumps: theory. J Colloid Interface Sci 268:133–142
9. Kang Y, Yang C, Huang X (2004) Analysis of the electroosmotic flow in a microchannel packed with homogeneous microspheres under electrokinetic wall effect. Int J Eng Sci 42:2011–2027
10. Yao S, Myers AM, Posner JD, Rose KA, Santiago JG (2006) Electroosmotic pumps fabricated from porous silicon membranes. J MEMS 15(3):717–728

Electropermeabilization

- ► Electroporation

Electrophoresis

KEVIN D. DORFMAN
Department of Chemical Engineering and Materials Science, University of Minnesota, Minneapolis, MN, USA
dorfman@umn.edu

Definition

Electrophoresis is the motion of charged particles in a fluid under the influence of an electric field.

Chemical and Physical Principles

Electrophoresis provides an important method of actuation in microfluidics. Many of the different types of species that need to be transported on a microfluidic device are charged, and electrophoresis thus provides a convenient method for moving them to different locations on a chip. Amongst the most important examples are colloidal particles, such as latex spheres, and biomolecules, such as proteins and DNA. Under certain circumstances, electrophoresis can also be used to separate these particles by zeta potential or size, which is an important part of biological analyses.

Electrophoresis also requires that the fluid entraining these particles be able to conduct electricity. Often, salts are added, yielding an electrolytic solution. The salts disassociate into positively charged ions (►cations) and negatively charge ions (►anions). The cations are attracted towards the negative electrode (the ►cathode) and anions are attracted towards the positive electrode (the ►anode). When dealing with biomolecules, the salts are usually weak acids and weak bases. The resulting solution is a buffer, which keeps the solution within a narrow pH range. As the charge and conformation of the biomolecules depend on the solution pH, the buffer composition plays an important role in biological applications of electrophoresis.

Consider first the simple case an isolated, charged ion moving in a uniform electric field, as illustrated in Fig. 1. While this is an overly simplistic picture of electrophoretic motion in solution, it serves to illustrate the general principle. We will consider a more realistic model of electrophoresis in free solution in the following section.

The ion possesses a charge Q, with $Q > 0$ for a cation and $Q < 0$ for an anion. The charge of the ion is given by the number of unpaired electrons or protons, with the elementary electric charge $e = 1.60219 \times 10^{-19}$ C per proton or electron. In this example, the ions in solution are assumed to be so dilute that they do not interact electrostatically. The ion is placed in a uniform electric field of strength E. The field strength is often reported in V/cm, although the proper SI units are V/m. In applications, one would typically apply a potential V between the two electrodes separated by a distance L. In this case, the electric field between them is simply

$$E = \frac{V}{L}. \tag{1}$$

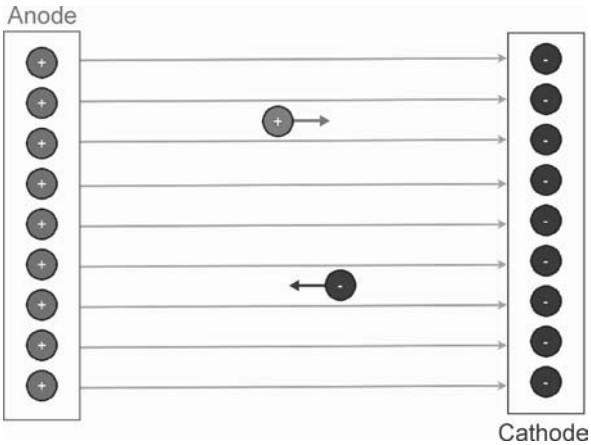

Electrophoresis, Figure 1 Electrophoresis of a cation and an anion in a uniform electric field. The anode and cathode are assumed to extend infinitely in the vertical direction to avoid end effects. The positively charged cations move towards the negatively charged cathode, whereas the negatively charged anions move towards the positively charged anode

The electrical force acting on the ion is the product of its charge and the electric field,

$$F_e = QE = \frac{QV}{L}. \tag{2}$$

For a nominal electric field of 10 V/cm acting on a monovalent ion (like Na^+), the electrical force would be 1.6×10^{-16} N – very small indeed! However, this force is sufficient to animate the ion because it is balanced by a very small drag force. If the ion is approximated as a spherical particle of radius a moving through a fluid of viscosity η, then the drag coefficient ξ is given by the Stokes drag

$$\xi = 6\pi\eta a, \tag{3}$$

and the drag force resisting the motion is

$$F_d = -\xi v. \tag{4}$$

By Newton's second law, the sum of the electrical force and the drag force equals zero. As a result, the ion has an electrophoretic velocity

$$v = \frac{QE}{\xi}. \tag{5}$$

Keeping the example of Na^+, the ionic radius is $a =$ 116 pm. If the electrophoresis is performed in a fluid with a viscosity similar to that of water (which is typically the case), then $\eta = 1$ cP $= 0.001$ Pa s, and the resulting drag coefficient is $\xi = 2.18 \times 10^{-12}$ Ns/m. With an electric force of 1.6×10^{-16} N, the sodium ion would thus

move at a speed of 73 μm/s. Albeit a very slow speed on macroscopic length scales, the ion moves over its own radius over 500,000 times per second.

In general, data are not reported as electrophoretic velocities, but rather as electrophoretic mobilities. The electrophoretic mobility is defined as

$$\mu \equiv \frac{v}{E}. \tag{6}$$

If the velocity is a linear response to the electric field, as is the case here, then the electrophoretic mobility is independent of the field. This scaling breaks down in the case of ►polyelectrolytes [1].

Determining the electrophoretic mobility of polyelectrolytes, such as colloidal particles and flexible polyelectrolyte chains such as DNA, is considerably more complicated because their electrostatics and hydrodynamics differ from the simple charged, spherical ion considered above. Polyelectrolytes are intrinsically uncharged, but contain ionizable groups (for example –OH and –H groups) that will dissociate from the particle when it is placed in solution. As indicated in Fig. 2, these ionizable groups, known as ►counterions, dissociate from the macroion. The dissociation is not limited by mass action, although flexible polyelectrolyte chains do not necessarily completely dissociate due to Manning condensation [2]. Note that the solution can also contain counterions and ►co-ions of its own (with co-ions having the same charge as the particle), which will normally be the case during electrophoresis in buffers. The overall system is electrically neutral – the number of counterions (red) equals the number of charges on the particle surface, and the number of counterions already in the solution (yellow) equals the number of solution co-ions (purple).

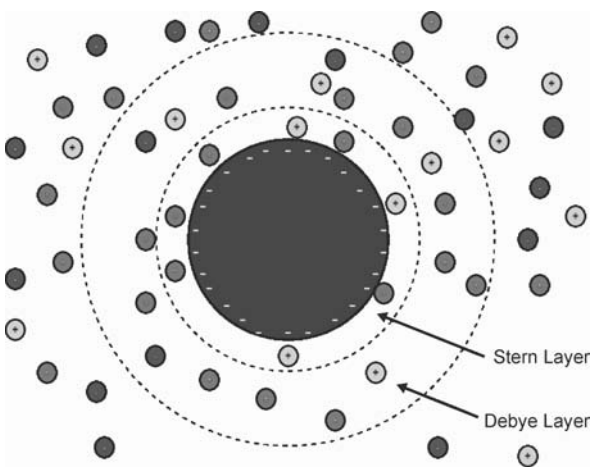

Electrophoresis, Figure 2 Polyelectrolytes contain ionizable groups that dissociate from the particle when it is placed in solution. In the figure, the red cations were originally associated with the colloidal particle. The yellow cations and purple anions represent the dissociated salts contained in the buffer solution. Nearby the particle, the counterions are strongly bound by electrostatics and chemical affinity for the colloid, leading to the formation of the Stern layer. The Stern layer is surrounded by a more diffuse layer of charges, known as the Debye layer, where the local density of counterions is governed by a balance between attraction towards the oppositely charged colloid, the repulsion from other counterions, and diffusion

When the counterions dissociate from the particle, diffusion attempts to randomize their locations. However, the counterions are attracted to the particle by electrostatic interactions, which act over long distances. Immediately proximate to the particle is a molecular-sized layer of counterions, called the Stern layer. The counterions in the Stern layer are immobile as a result of their chemical affinity for the particle surface, as well as the very strong electrical attraction at short distances from the charged particle. The Stern layer also includes polar water molecules that are oriented to the surface. A second, larger layer of charges, called the ►Debye layer, surrounds the Stern layer. These charges are mobile and their location is affected by electrostatic attraction to the sphere, which wants to pull them towards the inner edge of the Debye layer, and diffusion, which tries to randomize their locations. To further complicate the issue, the counterions repel one another, since they have the same charge. Exactly computing the structure of the Debye layer is a challenging task, requiring the solution of the nonlinear Poisson–Boltzmann equation (see ►Lattice Poisson-Boltzmann Method, Analysis of Electroosmotic Microfluidics), but the characteristic thickness can be obtained from scaling, yielding

$$\kappa^{-1} = \sqrt{\frac{\varepsilon_0 \varepsilon_b k_B T}{2e^2 I}}. \tag{7}$$

In the latter, ε_0 is the permittivity of vacuum (8.854×10^{-12} F/m) and ε_b is the permittivity of the bulk solution (or the dielectric medium), k_B is Boltzmann's constant (1.38×10^{-23} J/K), and T is the temperature in Kelvin. The parameter I is the ionic strength of the medium,

$$I = \frac{1}{2} \sum_i z_i^2 c_i, \tag{8}$$

where z_i is the valence of ion i and c_i is its concentration. The ►Debye length is historically written as an inverse length (i. e. κ has units of m^{-1}). In typical biological buffers, the Debye length is between 1 – 10 nm.

Key Research Findings

Free Solution Electrophoresis

The first key physical phenomenon to consider is the electrophoresis of colloidal particles and polyelectrolytes in free solution. The use of the term free solution here implies two assumptions: the particles are very far from any boundaries and the particles are sufficiently dilute so that they do not interact with one another. Free solution results are generally applicable for electrophoresis in an empty microchannel, provided that the particles are not too large relative to the smallest dimension of the channel. As a rule of thumb, the particle radius (or the radius of gyration, in the case of polyelectrolytes) should be at least one order of magnitude less than the smallest channel dimension. As systems move towards the nanoscale, the interactions with the walls (and other effects of confinement) will become increasingly important.

Consider first the electrophoresis of the colloidal particle of charge Q and radius a depicted in Fig. 3. As mentioned above, the particle dissociates into a single large, charged species (the macroion) and a number of small counterions. Since these species have different charges, they will move in opposite directions with respect to the electric field. Determining the electrophoretic mobility of a charged colloidal particle for an arbitrary Debye layer thickness is a daunting task. However, two simple limits can be computed relatively easily. The following two derivations follow very closely from Ref. [3].

In the case where the Debye layer is very large relative to the particle size, i. e. when $\kappa a \to 0$, then the counterions are distributed uniformly throughout space. As a result, their motion does not affect the motion of the colloidal particle and the electrophoretic mobility is given by Eqs. (5) and (6). We can further simplify this by noting that, for a spherical particle of total charge Q, Gauss's law requires that the particle's charge create an electric field

$$E = \frac{Q}{4\pi\varepsilon\varepsilon_0 r^2} \tag{9}$$

that decays like $1/r^2$ as we move away from a Gauss surface centered on and enclosing the particle. The potential ψ is related to the electric field by

$$E = -\nabla\psi\,. \tag{10}$$

In spherical coordinates, the potential at the surface of the particle is thus given by

$$\psi_s = \int_a^\infty E\,\mathrm{d}r\,, \tag{11}$$

where we have set the potential at infinity to be zero. Integrating, we find the potential to be

$$\psi_s = \frac{Q}{4\pi\varepsilon\varepsilon_0 a}\,. \tag{12}$$

If we assume that the drag on the sphere is given by Stokes Law,

$$\xi = 6\pi\eta a\,, \tag{13}$$

then substituting Eqs. (12)–(13) into Eq. (6) furnishes the mobility

$$\mu = \frac{2\varepsilon\varepsilon_0\psi_s}{3\eta}\,. \tag{14}$$

While Eq. (14) is aesthetically pleasing, it is not particularly useful in practice for two reasons. First, although we can define a surface potential ψ_s for our calculation, in general it is not possible to measure the surface potential directly. Second, the presence of adsorbed counterions and oriented water in the Stern layer leads to an immobile layer immediately proximate to the sphere. To circumvent these problems, we define a zeta-potential, ζ. The zeta potential is a phenomenological parameter, which is often associated with the electrical potential at the edge of the Debye layer closest to the particle surface. Alternatively, the zeta-potential can be defined as the potential at the so-called "shear plane," i. e. the point at which the fluid begins to move at a different velocity than the sphere. In

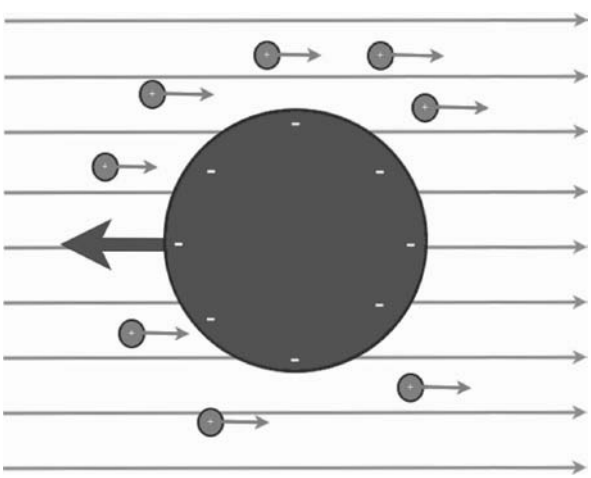

Electrophoresis, Figure 3 Schematic of the electrophoresis of a rigid colloidal particle. The electric field acts on both the counterions and the macroion, resulting in relative motion in opposite directions

principle, the zeta potential could be measured by electrophoresis through Eqs. (17) or (22), although it is normally determined by static methods (see ►zeta potential measurements).

As the Stern layer is quite thin, we can take the zeta-potential to be

$$\zeta = \psi(\delta + a)\,, \tag{15}$$

i. e. the potential ψ at some distance $a + \delta$ from the sphere center, where $\delta \ll a$. Returning to Eq. (11), we now have

$$\zeta = \int_{a+\delta}^{\infty} E\,\mathrm{d}r\,, \tag{16}$$

where the electric field E is still given by Eq. (9). Noting the thinness of the Stern layer relative to the particle size, the zeta potential is given approximately by Eq. (12), where upon the mobility in the infinite Debye layer limit is

$$\mu = \frac{2\varepsilon\varepsilon_0\zeta}{3\eta}\,. \tag{17}$$

The other simple result occurs in the opposite limit, $\kappa a \to \infty$, where the thickness of the Debye layer is very small relative to the size of the particle. This is particularly relevant for microfluidic applications in ionic buffers, which is the usual situation for bioanalyses. As the typical Debye layer thickness is several nanometers, the electrophoresis of any micron-sized particle will be governed by this limit.

Outside of the Debye layer, the fluid is electrically neutral. Inside the Debye layer, the fluid obeys the Navier-Stokes equation with an electrical body force

$$\eta\frac{\mathrm{d}^2u}{\mathrm{d}z^2} + \rho^{(e)}E = 0\,, \tag{18}$$

where $\rho^{(e)}$ is the space charge inside the Debye layer. The latter is related to the electrical potential via Poisson's equation,

$$\varepsilon\varepsilon_0\frac{\mathrm{d}^2\psi}{\mathrm{d}z^2} = -\rho^{(e)}\,. \tag{19}$$

Working in a reference frame that moves with the particle, we require that the fluid velocity at the edge of the Stern layer (where $\psi = \zeta$) vanish due to the no-slip condition. As a result, Eq. (18) and the no-slip condition are satisfied by the fluid velocity

$$u(z) = -\frac{\varepsilon\varepsilon_0}{\eta}[\zeta - \psi(z)]E\,. \tag{20}$$

At the edge of the Debye layer, the potential drops to zero. As a result the bulk fluid is moving at a velocity

$$u = -\frac{\varepsilon\varepsilon_0\zeta}{\eta}E\,, \tag{21}$$

since the body force appearing in Eq. (18) is zero outside of the Debye layer. If we switch our frame of reference and consider a particle moving in an otherwise quiescent fluid, then the particle moves in the opposite direction to the fluid with a mobility

$$\mu = \frac{\varepsilon_0\varepsilon_\mathrm{b}\zeta}{\eta}\,. \tag{22}$$

Equation (22) reveals an important feature of electrophoresis in the small Debye layer limit: the electrophoretic mobility is independent of the size of the particle. As a result, particles of any size will move at the same speed in free solution. This is a desirable feature when the goal is to move the particles to different locations on a chip. On the other hand, Eq. (22) implies that the common task of sorting colloidal particles by size cannot be accomplished by free-solution electrophoresis.

Now consider the case of flexible polyelectrolytes such as DNA. There are two dominant hydrodynamic models for polymer motion, the Rouse model and the Zimm model [4]. In the Rouse model, the different parts of the chain are assumed to be hydrodynamically independent, so that the total friction of the chain is simply the sum of the friction of each segment. The Rouse model is also referred to as freely draining, since the polymer chain appears to be hollow to the fluid. The Zimm model includes both the Rouse friction of the individual segments with the fluid and the hydrodynamic interactions between different segments. The Zimm model is not freely draining; the polymer appears as a solid object to the surrounding fluid.

During electrophoresis in free solution, polyelectrolytes are freely draining and exhibit Rouse-like behavior. The reason for the absence of hydrodynamic interactions during electrophoresis is the exponential decay of electrostatic effects; the very thin Debye layer surrounding the polyelectrolyte screens the hydrodynamic interactions and allows each segment to act individually [2]. Thus, if the chain consists of N segments with charge q per segment, the total electrical force acting on the chain is

$$F_\mathrm{e} = qNE\,. \tag{23}$$

Likewise, if the friction on each segment is given by ξ, then the total frictional force on the chain will be given by

$$F_\mathrm{f} = -N\xi v\,. \tag{24}$$

Noting that these two forces balance one another, and making use of the definition in Eq. (6), the electrophoretic mobility of long polyelectrolytes is thereby independent of molecular weight,

$$\mu = \frac{v}{E} = \frac{qN}{N\xi} \sim N^0 . \tag{25}$$

The free solution electrophoresis of long polyelectrolytes is thus qualitatively the same as colloidal particles; all chains will move at the same speed, independent of molecular weight. Note that the latter scaling for the mobility does not hold for the diffusion coefficient. Polyelectrolyte chains still diffuse with a molecular weight-dependent Zimm diffusivity [4].

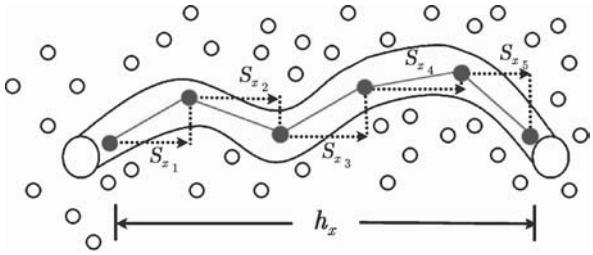

Electrophoresis, Figure 4 When a long polyelectrolyte like DNA is electrophoresed through a gel, the fibers of the gel confine the DNA to a reptation tube. The force acting on each segment of the tube depends on the orientation vector s_x of that segment in the electric field. The total projection of the chain, h_x, is the sum of the orientation vectors (Eq. (16)). The net velocity of the chain is computed from the average motion of the chain through many tubes, each of which has a different projection h_x

E

Gel Electrophoresis: Separating Polyelectrolytes by Size

The above discussion makes clear that colloidal particles and polyelectrolytes cannot be separated by size during free solution electrophoresis. As a result, many electrophoretic size separations for chemistry and biology are performed in gels. The precision afforded by microfabrication has led to miniaturized version of these classic protocols, as well as a number of novel separation techniques that differ distinctly from the separation principles prevailing in gels [5]. In order to best understand the current research in microfluidic separations of colloids and polyelectrolytes, in particular the important applications to protein and DNA separations, it is important to first understand the physics of gel electrophoresis.

For small particles, such as colloids and collapsed proteins, the dominant separation mechanism is Ogston sieving [1]. The underlying hypothesis behind the Ogston model is that the electrophoretic mobility is equal to the free volume available to that particle. In principle, this free volume argument should account for both the reduction in entropy due to excluded volume effects as well as the fact that large particles will run into "dead ends" in the gel. Although the Ogston hypothesis does not explicitly account for these effects, it nonetheless provides a useful model for the electrophoresis of globular particles in gels. The result of the model is that the mobility of a particle of size a in a gel of concentration c is given by

$$\frac{\mu(a,c)}{\mu(a,0)} = \exp[-K(a)c] , \tag{26}$$

where $K(a) \sim a + R_{\text{fiber}}$ is the retardation factor, with R_{fiber} the size of the gel fibers.

The precision of micro- and nanofabrication should allow this model to be tested in well-controlled systems. Indeed, theoretical work by Slater and coworkers has questioned the validity of the Ogston model through a number of studies of electrophoresis in regular arrays of obstacles (see [6] and subsequent papers in this series).

Although their free-solution behaviors are similar, flexible molecules (like DNA and denatured proteins) exhibit dramatically different behavior in a sieving matrix. Once the size of the pores in the gel becomes small relative to the radius of gyration of the polyelectrolyte chain, the polyelectrolyte chain must uncoil in order to move through the gel. Although the uncoiling process is entropically unfavorable (since it reduces the number of available conformations for the chain), the entropy loss is offset by the reduction in the electrical potential energy as the chain moves in the field.

The mobility of flexible chains in gels is well described by the biased reptation model [1], which is indicated schematically in Fig. 4. In the model, the fibers of the gel are coarse-grained into a ►reptation tube that confines the chain. The chain thus slithers along the tube contour (the reptation part) under the influence of the electric field, which provides a tendency for the slithering motion to be in the direction of the electric field (the biased part).

The electrophoretic mobility can be computed from the picture presented in Fig. 4. The electric field exerts a force $\hat{q}Es_x$ on each segment of the chain, which depends on the orientation s_x of the segment in the direction of the electric field and its charge per unit length, $\hat{q}$. The total electric force acting on the chain is the sum of the force acting on each segment,

$$F_e = \sum (\hat{q}E)s_x . \tag{27}$$

As indicated in Fig. 4, the total projection of the chain is given by

$$h_x = \sum s_x , \tag{28}$$

whereupon the total electric force is given by summing the forces over the whole chain,

$$F_e = QE\frac{h_x}{L}. \tag{29}$$

In the latter, Q is the total charge of the chain and L is its contour length. The curvilinear friction counters the electrical force,

$$F_f = -\xi_c v_c, \tag{30}$$

where ξ_c is the friction coefficient for motion along the contour at a velocity v_c. Balancing the friction against the electrical force, the velocity along the tube contour is thus

$$v_c = \frac{F}{\xi_c} = \frac{QEh_x}{\xi_c L} = \frac{\mu_0 E h_x}{L}, \tag{31}$$

where the free solution mobility μ_0 is defined to be $\mu_0 = Q/\xi_c$, analogous to Eq. (6). The time required to move through the tube is

$$t = \frac{L}{v_c}, \tag{32}$$

during which time the chain has moved a distance h_x in the direction of the field. As a result, the velocity in the x-direction through a tube with an extension h_x is

$$v_x = \mu_0 E\left(\frac{h_x}{L}\right)^2. \tag{33}$$

After the motion through many such tubes, the electrophoretic mobility is given by the average of the velocity in each tube divided by the field,

$$\frac{\mu}{\mu_0} = \frac{\langle h_x^2\rangle}{L^2}, \tag{34}$$

where $\langle\cdots\rangle$ represents the average over many tubes.
Albeit overly simplistic [1], the analysis leading to Eq. (34) qualitatively captures much of the key phenomena observed experimentally. As indicated in Fig. 5, when the field acting on the chain is weak, then the chain is not strongly deformed and retains its Gaussian conformation (with a size proportional to $L^{1/2}$). The average conformation is thus a random walk. The reptation tubes have the average extension

$$\langle h_x^2\rangle \sim L, \tag{35}$$

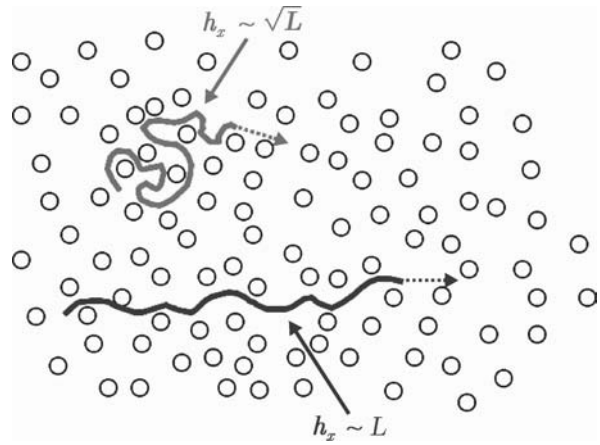

Electrophoresis, Figure 5 Illustration of biased reptation with and without orientation. For weak fields and small chains (as indicated in the upper red figure), the electric field does not strongly perturb the conformation of the chain and it remains in a Gaussian coil. The projection of the coil in the direction of the field thus scales like $L^{1/2}$ for a chain of length L. For long DNA or strong fields (as indicated in the lower blue figure), the chain tends to be come oriented in the direction of the electric field. The projection of the chain then scales like its total length L

and the mobility depends on molecular weight. If the field is strong, then the chain is strongly extended and the tubes are almost fully extended and

$$\langle h_x^2\rangle \sim L^2. \tag{36}$$

As a result, the separation is lost and all chains will move at the same speed. These scaling results agree well with experiments, and the so-called compression band, where all of the long chains co-migrate, is a major limitation of gel electrophoresis. As a result, a great deal of effort in microfluidics and nanofluidics research has focused on designing systems which permit the separation of long DNA and other polyelectrolyte chains by methods other than biased reptation.

The Joule Heating Problem and Applying Microscale Electric Fields

In addition to the difficulties in electrophoretically separating particles by size, a second challenge in electrophoresis is Joule heating. The heat generated by a conducting solution is given by Joule's law,

$$W_{Joule} = \sigma E^2 \tag{37}$$

where σ is the conductivity of the fluid. Heating can be catastrophic for electrophoretic processes; non-uniform changes of temperature lead to viscosity gradients, which

in turn result in strong convective currents that can overwhelm the electrophoretic motion. In practice, Joule heating leads to a smearing of the separation bands (or a single plug of solute) and limits the maximum electric field that can be applied.

Microfluidics and nanofluidics offer an excellent solution to the Joule heating problem. The Joule heat must be removed from the system by thermal diffusion. The diffusive heat flux for a temperature drop ΔT across a channel of size w is given by

$$W_{\text{diff}} \sim k\frac{\Delta T}{w^2}\,, \tag{38}$$

where k is the thermal conductivity of the solution. If these two heat fluxes [Eqs. (37) and (38)] are balanced, then the maximum permissible electric field scales like the inverse of the channel width. As a result, much higher electric fields (and thus faster electrophoretic velocities) are possible as the channel sizes are reduced. As microfluidic and nanofluidic systems also require transporting the solute over small distances, the total gain in process speed can be significant.

Joule heating is not the only problem associated with applying strong electric fields. In typical microsystem applications, the electric field is applied via platinum electrodes inserted into the various reservoirs on the chip. The application of the field leads to electrolysis of the water (i. e., the dissociation of water into oxygen and hydrogen) and bubble formation. When large reservoirs are used, the bubbles are generally not troublesome because they will rise to the top of the reservoir and exit the system. Indeed, electrolysis and Joule heating have long been recognized as problems in conventional gel electrophoresis, but the large size of the system and buffer recirculation can relieve the problem to some extent. These are not options for microsystems. When small reservoirs are used or the electrodes are located inside a channel system, the resultant bubble formation can be catastrophic. The bubbles are very difficult to remove from the system, clogging the channels and causing sharp changes in the channel current.

Examples of Application

Electrophoretic separation of small charged species was one of the earliest applications of Lab-on-a-Chip and microfluidics. Indeed, the paper [7] that introduced the term μTAS (micro-total analysis system) dealt primarily with the electric field limits imposed by Joule heating. Microfluidic electrophoresis leads to tremendous gains in the separation time and strongly reduces the amount of sample consumed on chip.

Microfluidics and nanofluidics have also lead to a number of new separation techniques for long DNA that circumvent the limits of gel separations [5]. One of the simplest approaches is to make an artificial gel by microfabricating an array of posts [8]. In this strategy, the post diameters are commensurate with the radius of gyration of the long DNA ($\sim 1\,\mu$m), whereas the posts are spaced by several microns. As a result, the DNA no longer needs to unwind and reptate through the artificial gel. Rather, the motion is governed by a cyclic process of collisions with the posts, unraveling and unhooking of the chain in a rope-over-pulley process, and then motion towards the next post. These dynamics are referred to as geometration, because they resemble the motion of an inchworm, and the motion can be analyzed by continuous time random walk theory [9]. Post arrays are but one example of the different electrophoretic separation techniques that have been proposed [5].

Cross References

- ► Lattice Poisson-Boltzmann Method, Analysis of Electroosmotic Microfluidics
- ► Dielectrophoresis
- ► Electrokinetic Motion of Cells and Nonpolarizable Particles
- ► Electrokinetic Motion of Heterogeneous Particles
- ► Electroosmotic Flow (DC)
- ► AC Electro-Osmotic Flow
- ► Electrophoretic Transport in Nanofluidic Channels
- ► Two-Dimensional Electrophoresis
- ► Zeta Potential Measurement

References

1. Viovy JL (2000) Electrophoresis of DNA and other polyelectrolytes: Physical mechanisms. Rev Mod Phys 72:813–872
2. Manning GS (1978) The molecular theory of polyelectrolyte solutions with applications to the electrostatic properties of polynucleotides. Quart Rev Biophys 11:179–246
3. Russel WB, Saville DA, Schowalter WR (1989) Colloidal Dispersions. Cambridge University Press, Cambridge
4. Doi M, Edwards SF (1986) The Theory of Polymer Dynamics. Oxford University Press, Oxford
5. Slater GW, Guillouzic S, Gauthier MG, Mercier JF, Kenward M, McCormick LC, Tessier F (2002) Theory of DNA electrophoresis ($\sim$ 1999–2002½). Electrophoresis 23:3791–3816
6. Slater GW, Guo HL (1996) An exactly solvable Ogston model of gel electrophoresis: I. The role of symmetry and randomness of the gel structure. Electrophoresis 17:977–988
7. Manz A, Graber N, Widmer HM (1990) Miniaturized total chemical analysis systems: a novel concept for chemical sensing. Sensors and Actuators B 1:244–248
8. Volkmuth WD, Austin RH (1992) DNA electrophoresis in microlithographic arrays. Nature 358:600–602

9. Minc N, Viovy JL, Dorfman KD (2005) Non-Markovian transport of DNA in microfluidic post arrays. Phys Rev Lett 94:198105

Electrophoresis of the Second Kind

Synonyms

Nonlinear electrophoresis; Superfast electrophoresis

Definition

Electrophoresis of the second kind refers to the nonlinear electrokinetic motion of a conducting particle passing a superlimiting current, due to electro-osmotic flow of the second kind.

Cross References

- ► Electrical Double Layers
- ► Electrokinetic Motion of Polarizable Particles
- ► Electroosmotic Flow (DC)
- ► AC Electro-Osmotic Flow
- ► Electrophoresis
- ► Electroosmosis of the Second Kind
- ► Induced-Charge Electro-Osmosis
- ► Induced-Charge Electrophoresis
- ► Nonlinear Electrokinetic Phenomena
- ► Super-Limiting Current

Electrophoretic Flow

- ► Electrophoretic Transport in Nanofluidic Channels

Electrophoretic Mobility

Definition

Velocity acquired by an ion per unit applied electric field.

Cross References

- ► Electrokinetic Flow and Ion Transport in Nanochannels

Electrophoretic Transport in Nanofluidic Channels

SUBRATA ROY[1], HARIBALAN KUMAR[2], RAMESH AGARWAL[3]

[1] Department of Mechanical and Aerospace Engineering, University of Florida, Gainesville, IA, USA
[2] Seamans Center for the Engineering Arts and Sciences, University of Iowa, Iowa City, IA, USA
[3] Aerospace Research and Education Center (AeREC) and Aerospace Engineering Program, Washington University, St. Louis, MO, USA
roy@ufl.edu, haribalan-kumar@uiowa.edu, rka@me.wustl.edu

Synonyms

Ion transport; Electrophoretic flow

Definition

The motion of electrically charged particles or molecules in a stationary medium under the influence of an electric field is called electrophoresis. In such transport the electric force is applied through a potential difference between electrodes. Selective use of the Lorentz force by applying a magnetic field can also induce such movement. Electrophoresis and electroosmosis are two key modalities of electrokinetic transport which are very useful in micro- and nanofluidics for a variety of applications including biomedical (bio-NEMS, etc.), fuel cell and micro total analysis systems (μ-TASs). In electroosmosis the bulk fluid moves due to the existence of a charged double layer at the solid–liquid interface. While one-dimensional electrophoresis is more commonly used, two-dimensional electrophoresis may also become a useful tool for the separation of gel proteins based on isoelectric property.

Overview

Let us consider an aqueous solution of a salt. A fraction of the salt dissociates into ions. Negatively charged ions are called anions, while positive ions are called cations. Such an ionic solution is called an electrolyte. If two electrodes are kept at a potential gap in such an electrolyte, the dissociated ions migrate towards oppositely charged electrodes at their characteristic speeds. Anions move towards the positive electrode, while cations are attracted by the negative electrode. The velocity and the number density of ions directly influence the electric current which increases with the strength of the electric field. Similar transport can also occur in a protein mixture that contains several charged species based on its degree of acidity. Chemical and electrical interactions may also occur during such transport. The electrons move across the electrochemical interface between the electrode and the electrolyte. The study of such migration of charged particles with or without the